Int J Earth Sci (Geol Rundsch) (2015) 104:587–601
DOI 10.1007/s00531-014-1106-6

ORIGINAL PAPER

Structural evidence for slip partitioning and inclined dextral transpression along the SE Sanandaj–Sirjan zone, Iran

Shahram Shafiei Bafti · Mohammad Mohajjel

Received: 15 April 2014 / Accepted: 14 November 2014 / Published online: 29 November 2014

Abstract The structural evolution of the Sanandaj–Sirjan zone is the result of the convergence of the Iranian microcontinent and the Afro-Arabian continent. The study area at Khabr in the SE Sanandaj–Sirjan zone, in the hinterland of the Zagros orogen, consists of Paleozoic, Mesozoic and Cenozoic rocks. In this area, deformation phases were distinguished in different rock units based on structural and stratigraphical evidence, and the deformational events are divided into two stages: (1) a Late Triassic event and (2) a Late Cretaceous to Miocene event. The Late Triassic deformation event caused regional metamorphism in the Paleozoic units. These units are overlain by unmetamorphosed Jurassic clastic sequences. Fabrics and structural evidence confirm that the F_1 folding recumbent and refolded folds were synchronous with the metamorphism of the Paleozoic units and terminated in the Early Jurassic. The time table of the orogenic phases shows that this deformation event is related to the Cimmerian orogenic phase. From a geodynamic point of view, the early Cimmerian deformation in the southeastern Iranian margin suggests that the SE Sanandaj–Sirjan zone was an active margin at that time. The early Cimmerian discordance recorded the onset of a contractional component related to the oblique subduction of Neo-Tethys beneath the central Iranian microcontinent. Structures related to the Late Cretaceous to Miocene deformation phase are observed in Jurassic to Oligocene units, which contain moderately inclined and plunging folds. Comparing these folds with domains of deformation generated in models of transpression shows that the folding was caused by a combination of contractional and dip-slip components of movement, eventually resulting in the formation of a thrust system. The Khabr thrust systems consist of five sheets of oblique thrusts, duplex structures and shear zones. The shear zones generally strike E–W and dip moderately N (30°–40°). The occurrence of asymmetric folds with hinges that are either parallel to strike or plunge down dip demonstrates an oblique-slip component in these thrust shear zones. The stretching lineation in the mylonites within the shear zones is defined by the long axes of ellipsoidal grains of quartz, calcite, plagioclase and garnet. In general, stretching lineations trend from N40°W to N80°W with an intermediate (35°) plunge. The geometry of foliation and lineation within these shear zones shows the effect of dip- and oblique-slip shearing. Deformation continued with strike-slip faulting becoming important during the last stages of deformation from the Miocene to the present day. The results of this study demonstrate that the evolution of the SE Sanandaj–Sirjan zone, from Late Triassic to Miocene, is compatible with an inclined dextral transpression along this zone.

Keywords Inclined dextral transpression · SE Sanandaj–Sirjan zone · Khabr area · SE Iran

S. Shafiei Bafti (✉)
Department of Geology, Faculty of Sciences,
Shahid Bahonar University of Kerman, Kerman, Iran
e-mail: Shafiei_Shahram@uk.ac.ir

M. Mohajjel
Department of Geology, Faculty of Sciences,
University of Tarbiat Modarres, Tehran, Iran

Introduction

Transpression is described in terms of the simultaneous action of strike-slip shearing and shortening normal to the shear zone (Harland 1971) and is considered to be an important style of deformation in regions of oblique convergence (Sanderson and Marchini 1984; Teyssier et al.

1995; Robin and Cruden 1994; Dewey et al. 1998; Lin et al. 1998; Jones et al. 1997, 2004; Díaz Azpiroz and Fernández 2005). The inclined transpression model involves the simultaneous action of pure shearing, strike-, and dip-slip shearing, resulting in triclinic flow (Jones et al. 2004).

Transpressional structures have been identified in the field in various parts of the Zagros orogen (Fig. 1) (Mohajjel and Fergusson 2000; Mohajjel et al. 2003; Agard et al. 2005; Authemayou et al. 2006, 2009; Sarkarinejad and Azizi 2008; Sarkarinejad et al. 2008). Structural analysis in the Neyriz area (Sheikholeslami et al. 2008) demonstrates oblique subduction for closing the Neo-Tethys. Structural evidence for transpression has also been recorded from the High Zagros (Fig. 1) in the Zagros collision zone (Agard et al. 2005; Authemayou et al. 2006; Axen et al. 2010). Dextral, brittle, transpressional deformation has been demonstrated from analysis faults in the Chadegan region of the Sanandaj–Sirjan zone (Babaahmadi et al. 2012). The paths of the relative motions of Arabia and Eurasia can be reconstructed from the brittle deformation in the Fars area of the Zagros (Navabpour et al. 2007) and have changed as follows: N030° (56–33 Ma), N025° (33–19 Ma), N009° (19–10 Ma) and N005° (last 10 Ma). Despite uncertainties in these kinematic reconstructions, the results strongly support a significant counterclockwise rotation of Arabia with respect to Eurasia since the Early Oligocene.

Oblique convergence in the Zagros collision zone is confirmed by measurements of the active tectonics (Vernant et al. 2004). GPS data indicate that the Arabian and Eurasian plates are currently converging at a rate of 21 mm/

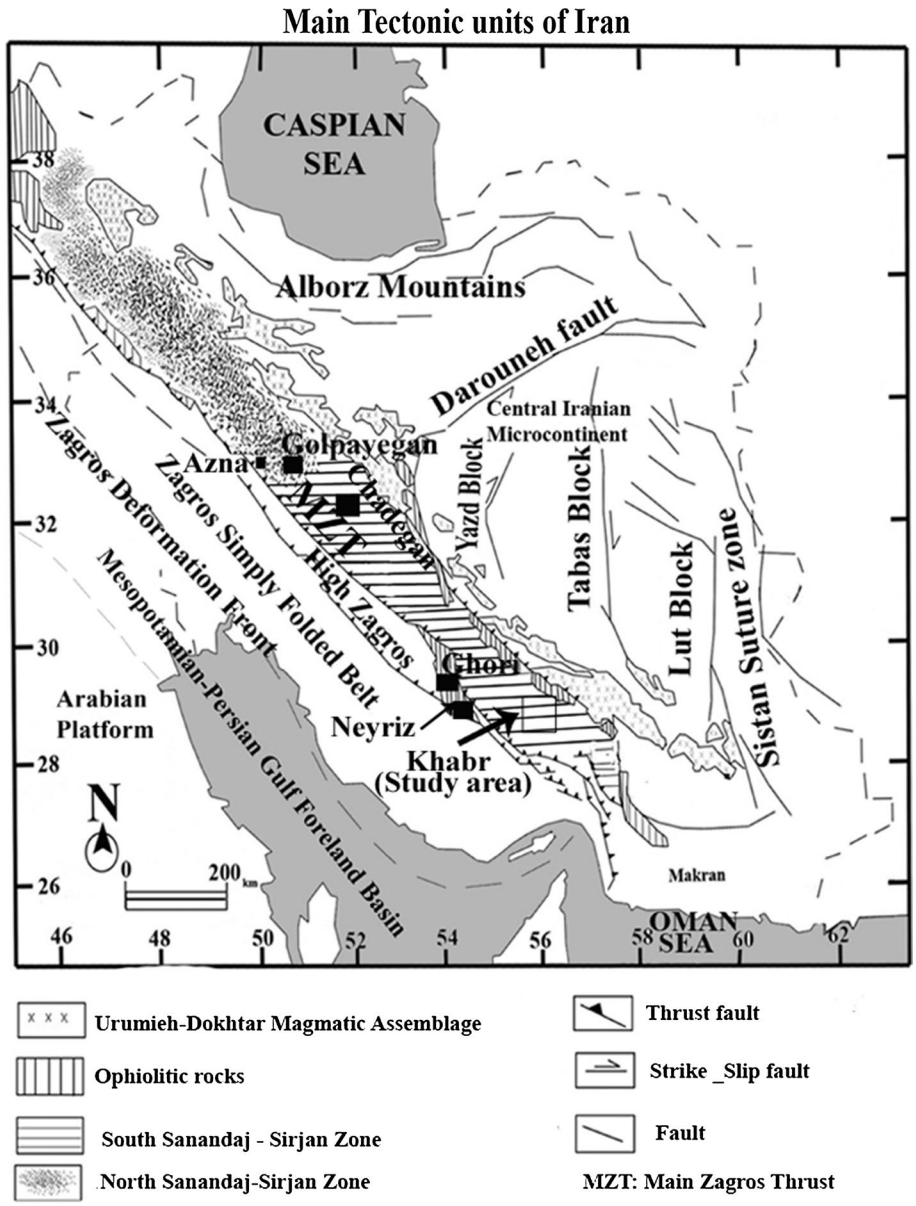

Fig. 1 Simplified tectonic map of Iran. The Sanandaj–Sirjan zone is located between the Urumieh–Dokhtar magmatic arc and the Zagros fold–thrust belt

year in the direction N050°. The shortening direction of the Zagros belt trends NNE–SSW, and the rate is 7 ± 2 mm/year, implying oblique convergence (Vernant et al. 2004). Transpression in the Zagros orogen was produced by oblique subduction and subsequent collision of the Arabian plate and the Iranian microcontinent. In the hinterland of the Zagros orogeny, in the June area (northern Sanandaj–Sirjan zone, Fig. 1), Mohajjel and Fergusson (2000) suggested oblique convergence at an angle of $\alpha = 70°$. In the Ghouri, Heneshk and Dehbid areas (southern Sanandaj–Sirjan zone), Sakarinejad (2007), Sarkarinejad and Azizi (2008) and Sarkarinejad et al. (2008) demonstrated an inclined dextral transpression with and angle $\alpha = 25°$. This shows considerable change of obliquity from NW to SE along the Sanandaj–Sirjan zone.

We have mapped structures in the Khabr area, in the SE part of the Sanandaj–Sirjan zone, and found evidence for both pure-shear and simple-shear deformation. Here, we describe structures that establish components of contraction, dip- and strike-slip that have resulted from pure-shear and simple-shear deformation. We interpret these structures in terms of a model of inclined dextral transpression for the SE Sanandaj–Sirjan zone.

Tectonic setting of Sanandaj–Sirjan zone

The Zagros orogen originated from the closure of the Neo-Tethys following the complete consumption of oceanic crust along a NE-dipping subduction zone and subsequent continental collision between the Afro-Arabian and Iranian continental fragments (Berberian and King 1981; Alavi 1994; Mohajjel and Fergusson 2000, 2014; Mohajjel et al. 2003; Agard et al. 2005, 2011). This orogenic belt consists of several parallel tectonic zones. These are from SW to NE: (1) the Mesopotamian–Persian Gulf foreland basin; (2) the Zagros fold–thrust belt, that itself is subdivided into three units from SW to NE: (a) the Zagros simply folded belt (Falcon 1967), which consist of ca. 13–14 km of shelf deposits of Permo-Triassic to Late Cretaceous/Paleocene age similar to those of Arabian plate, (b) a more complex pattern of sedimentation up to the recent Pliocene and (c) crush zone or High Zagros with imbricate slices comprising Mesozoic limestone, radiolarites, obducted ophiolite remnants and Eocene volcanics and turbidites, which are all thrust onto the Zagros fold–thrust belt; (3) the Sanandaj–Sirjan zone (Stöcklin 1968); and (4) The Urumieh–Dokhtar magmatic arc. The two major parallel domains of the Sanandaj–Sirjan zone and Urumieh–Dokhtar magmatic arc, to the northeast of the Main Zagros Thrust, are presumed to be the result of a northeast-dipping subduction process linked to the subduction of Neo-Tethyan oceanic crust beneath Iranian continental active margin (Berberian and King 1981; Alavi 1994; Omrani et al. 2008; Agard et al. 2011). The Sanandaj–Sirjan zone contains weakly to intensely deformed and metamorphosed rocks and represents the hinterland of the Zagros Orogen (Mohajjel and Fergusson 2000; Sheikholeslami et al. 2008).

The Sanandaj–Sirjan zone is separated from the Zagros fold–thrust belt by the Main Zagros Thrust in the southwest and is bordered by the Urumieh–Dokhtar magmatic arc in the northeast (Fig. 1). It has a width of 150–250 km and a length of 1,500 km, stretching from SE Iran to NE Iraq where it joins the Taurus belt in Turkey. The rocks in the Sanandaj–Sirjan zone are mostly of Mesozoic age; Paleozoic rocks are rarely exposed in the NW section of this zone but are common in the southeast (Berberian and King 1981). The Sanandaj–Sirjan zone is characterized by metamorphic and complexly deformed rocks and contains abundant deformed and undeformed Mesozoic plutons, in addition to widespread Mesozoic volcanic rocks (Mohajjel et al. 2003). The zone has been subdivided into a northern and southern part (Fig. 1) (Eftekharnejad 1981; Ghasemi and Talbot 2006; Arfania and Shahriari 2009). The northern Sanandaj–Sirjan zone is dominated by Triassic–Jurassic rocks, but in places, Cretaceous turbidites, originally deposited as deep submarine fans, are preserved and intruded by plutons. The northern part of the zone was deformed and metamorphosed in the Late Jurassic–Early Cretaceous. Green-schist facies metamorphism was accompanied by the intrusion of felsic granitoid plutons, including the Borojerd and Alvand (Mahmoodi et al. 2011; Ahmadi Khalaji et al. 2007; Ghalamghash et al. 2009). In this part of the Sanandaj–Sirjan zone, evidence for Jurassic–Early Cretaceous deformation and metamorphism is provided by unconformities in the Golpayegan area (Mohajjel et al. 2003). The Southern part consists of both Paleozoic rocks that formed in an epicratonic setting and a Carboniferous–Permian mafic and ultramafic complex (253–279 Ma; Ghasemi 2001). In the south Sanandaj–Sirjan zone, the Paleozoic units were deformed and metamorphosed during the early Cimmerian orogeny in the Late Triassic and an unconformity exists between the Paleozoic and the Jurassic units in the Khabr and Faryab areas (GSI 1997b; Arfania and Shahriari 2009; Shafiei et al. 2011). Structures associated with the early Cimmerian orogenic phase are south-southwest verging folds deformed under low-grade green-schist metamorphic conditions. The early Cimmerian deformation which developed along the southern Iranian margin suggests that it acted at that time as an active margin (Berberian and King 1981; Mohajjel et al. 2003; Sheikholeslami et al. 2008).

Late Jurassic–Early Cretaceous tectonic events in the Sanandaj–Sirjan zone were followed by deposition of continental clastic rocks (Stöcklin 1968; Berberian and King 1981) that are overlain by Early-to-Middle Cretaceous

carbonates. Late Cretaceous and/or younger volcanoclastic rocks are also found in the northern Sanandaj–Sirjan zone (Alavi 1994). During the Late Oligocene–Early Miocene, the marine carbonates of the Qom Formation accumulated along the northwestern Sanandaj–Sirjan zone.

The Sanandaj–Sirjan zone contains an outer belt of imbricate thrust slices that includes the Zagros suture and an inner belt of Paleozoic–Mesozoic poly-folded metamorphic rocks (Mohajjel et al. 2003). Regional deformation of the southern Sanandaj–Sirjan zone in the Late Triassic and the northern Sanandaj-Sirjan zone in the Late Jurassic produced pervasive southwest verging, northwesterly trending fold structures accompanying green-schist facies metamorphism (Mohajjel and Fergusson 2000; Mohajjel et al. 2006). This convergent deformation was related to crustal thickening along the active margin of the northeastern Sanandaj–Sirjan zone. Structural analysis in the adjoining low-grade metamorphic rocks and deformed silicic igneous rocks in Dorud–Azna region (Fig. 1) indicates that this deformation was produced in an episode of dextral transpression with low obliquity (Mohajjel and Fergusson 2000).

The timing of collision has been debated in the published literature in contrast to the timing for the initiation of subduction of the Neo-Tethys. All researchers agree that subduction was initiated prior to the Middle Jurassic, but the timing was not consistent throughout the Sanandaj–Sirjan zone (Mohajjel et al. 2003). Stratigraphy and structural evidence indicate that subduction closed diachronously from the SE to the NW (Sheikholeslami et al. 2008; Shafiei et al. 2011).

The timing of collision is still widely debated with Alavi (1994, 2004) arguing for Late Cretaceous initiation of collision, beginning with emplacement of ophiolite complexes that are exposed along the Zagros suture zone (Fig. 1). Many authors have argued that continental collision was in the Cenozoic with estimates ranging from the Paleocene–Late Eocene to Late Miocene (e.g., Berberian and King 1981; Mohajjel et al. 2003). Global reconstructions show that a wide seaway existed along the Zagros orogen until the mid-Cenozoic (Ricou 1994; Sengor and Natalin 1996; McQuarrie et al. 2003; Golonka 2004). A Paleocene to Early Eocene timing of collision was favoured by Ghasemi and Talbot (2006) and argued by Mazhari et al. (2009) on the basis of Eocene bimodal plutonic rocks, which are considered to be post-collisional. On the basis of structural and stratigraphic relationships in northwestern Iran, Agard et al. (2005) argued for collision prior to 23–25 Ma. Closure of the Tethys seaway along the Zagros connecting the widening Indian Ocean with the Mediterranean Sea occurred in the Miocene around 15 Ma (Woodruff and Savin 1989). A younger timing in the Late Miocene has been advocated by McQuarrie et al. (2003). The same argument occurs for the Indian–Asian collision (Aitchison et al. 2007).

Rock units in the study area

The study area (Fig. 2) contains successions of Lower Paleozoic to Mesozoic and Cenozoic units. Paleozoic strata are subdivided into two complexes: (l) the Cambrian Gol-e-Gohar complex (P_{Z2}, Pzgn), dominated by amphibolite, mica schist, gneiss and quartzite which, according to a geological map of the area (GSI 1997b), is equivalent to the Lalun Formation in central Alborz (N Iran); (2) the Ordovician Routshun Complex (P_{Z3}, Pzm_3) that consists of marble, meta dolomite, green schist and mica schist. Paleontological studies have established that these units are Lower Paleozoic in age and the equivalents of the Mila Formation in central Alborz (GSI 1997a). These Paleozoic units are unconformably overlain by Mesozoic strata, which are subdivided into two complexes: (l) the Early-to-Middle Jurassic Abkhamosh complex (J_f), consisting of shale, sandstone and conglomerate covered by andesitic and basaltic flows (Jv), and (2) the Late Jurassic to Early Cretaceous Kahdan complex (Jkmv and Jkmt), dominated by thick layers of sandstone, conglomerate and basaltic and andesitic flows. To the south of the Khabr thrust fault (T2) (Fig. 2), the Kahdan complex appears as an olistostrome containing blocks from the Routshun complex (GSI 1997b). Cenozoic strata consist of Eocene–Oligocene turbidites (E^{wf}, E^{f}, E^{c} and O) that contain conglomerates, shales and nummulitic sandstone. These units crop out north of the T2 thrust fault (Fig. 2). The Paleozoic units are intruded by a suite of Late Triassic granitic plutons in the SE Sanandaj–Sirjan zone (Berberian and Berberian 1981) and occur in the southern part of the study area (Fig. 2).

Structural architecture

In the SE Sanandaj-Sirjan zone, Jurassic conglomerate and sandstone uncomformably cover folded Paleozoic metamorphic complexes. This stratigraphic relationship reflects the early Cimmerian phase (Late Triassic) of deformation and metamorphism in the Paleozoic complexes in the SE Sanandaj–Sirjan zone. Similar evidence was also documented west of Sirjan (Berberian and King 1981), the Dehsard area (GSI 1997b), the Faryab area (Shafiei et al. 2011) and the Quri-Kor-e-Sefid area (Sheikholeslami et al. 2008). It is important to note that the metamorphic grade and the style of deformation in the Paleozoic complexes are not the same as the Mesozoic and Tertiary rock units.

It is suggested that the style of deformation and metamorphism is divided into the Late Triassic deformation stage that effected Paleozoic rocks and a Late

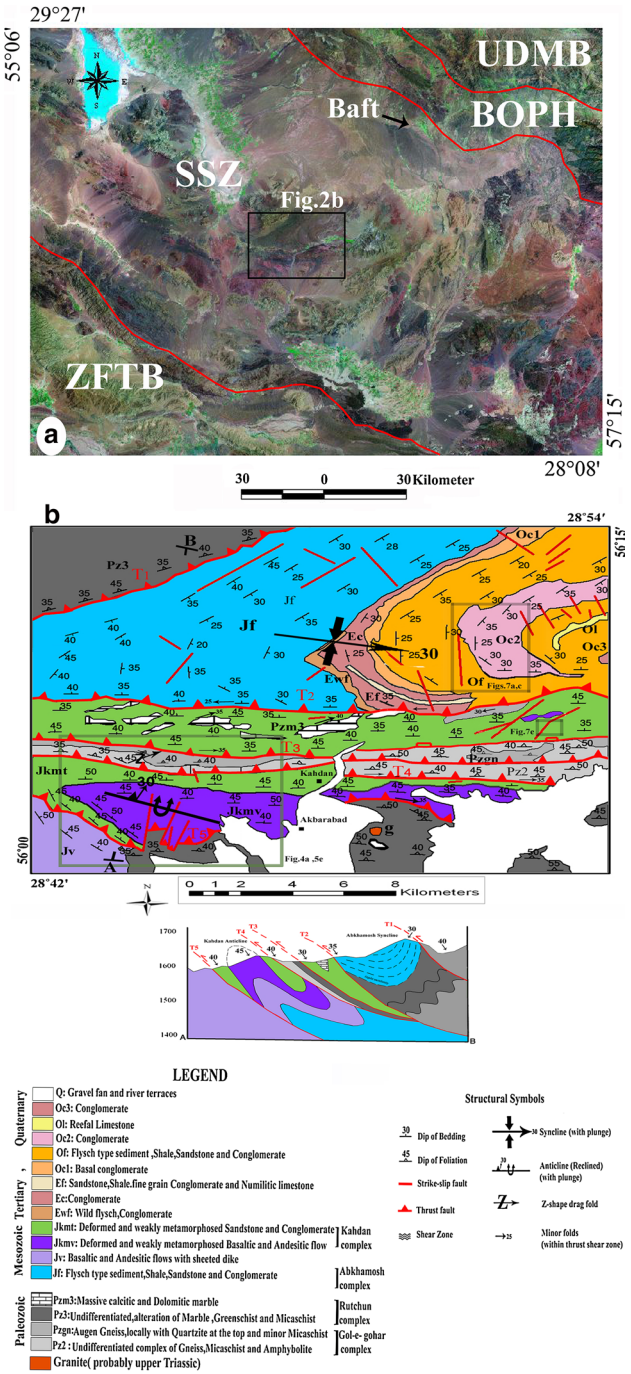

Fig. 2 **a** Satellite image from MrSID; multi-resolution seamless image database which is a patented, wavelet-based file format designed to enable portability of massive bit-mapped (*raster*) images showing the geological setting of the study area (*inset box*) in the southeastern part of the Sanandaj-Sirjan zone (*UDMB* Urmieh–Dokhtar magmatic belt, *BOPH* Baft ophiolite, *SSZ* Sanandaj–Sirjan zone, *ZFTB* Zagros fold–thrust belt. **b** Major structures and rock units in the study area

Cretaceous–Miocene deformation stage that is observed in the younger rocks. Here we describe the geometry and kinematics of the deformation stages in more detail.

Late Triassic deformation stage

D_1 deformation

The D_1 deformation phase produced F_1 folds and S_1 axial plane foliation. They are common in schist and marble in the Gol-e-Gohar and Routshun complexes (GSI 1997b) to the east of Akbarabad (Figs. 2b, 3a, b). F_1 folds show isoclinal profiles, and orientation that varies from moderately inclined to recumbent axial planes (AP_1) strike E–W and dip gently (10°–15°) to the north, and fold axes plunge at 10°–20° E. Within schist, S_1 foliation is marked by syntectonic growth of muscovite and biotite flakes, recording green-schist/amphibolite metamorphic facies conditions. S_1 foliation is generally oriented E–W and dips moderately to the N (Fig. 3d).

D_2 deformation

The D_2 deformation resulted in coaxial refolding of F_1 folds. F_1 axial planes (AP_1) are strongly folded. Superposition of F_1 and F_2 produced type III interference patterns as described by Ramsay and Huber (1987) (Fig. 3a–c). These patterns crop out in the Routshun complex to the east of Akbarabad. Within schist and the thin-layered marble of the Gol-e-Gohar and Routshun complexes, the D_2 deformation generated a crenulation cleavage. S_1 and S_2 show a sequence of foliation development in the green schist and garnet-mica schist. In the garnet-mica schist, garnet crystals show a straight inclusion trail and the internal foliation makes an angle with external foliation of about 50°. This crystal is interpreted having grown between D_1 and D_2 (Fig. 3e–g).

Late Cretaceous–Miocene deformation stage

D_3 deformation

This deformation is represented by folds, thrusts and related shear zones. These folds crop out in the Jurassic, Cretaceous (Abkhamosh and Kahdan complexes) and Oligocene–Miocene rock units. In the Abkhamosh complex and Oligocene–Miocene rock units, folds are steeply inclined, axial plane dip 75°–80° SW, and a syncline plunges 30°–35° to the SE (Fig. 4a, b). In the Kahdan complex, the fold is reclined, the axial plane dips 30°–35° to the NE, and an anticline plunges 30° to the NNE (Fig. 4c, d).

S_3 foliation is developed parallel to the folds axial planes and commonly parallel to the bedding on the limbs of folds. S_3 is a deformation fabric but not a metamorphic structure. Within the deformed andesitic and basaltic units, S_3 is defined by the alignment of primary amphibole and pyroxene, rotated around plagioclases, and within the shale, and

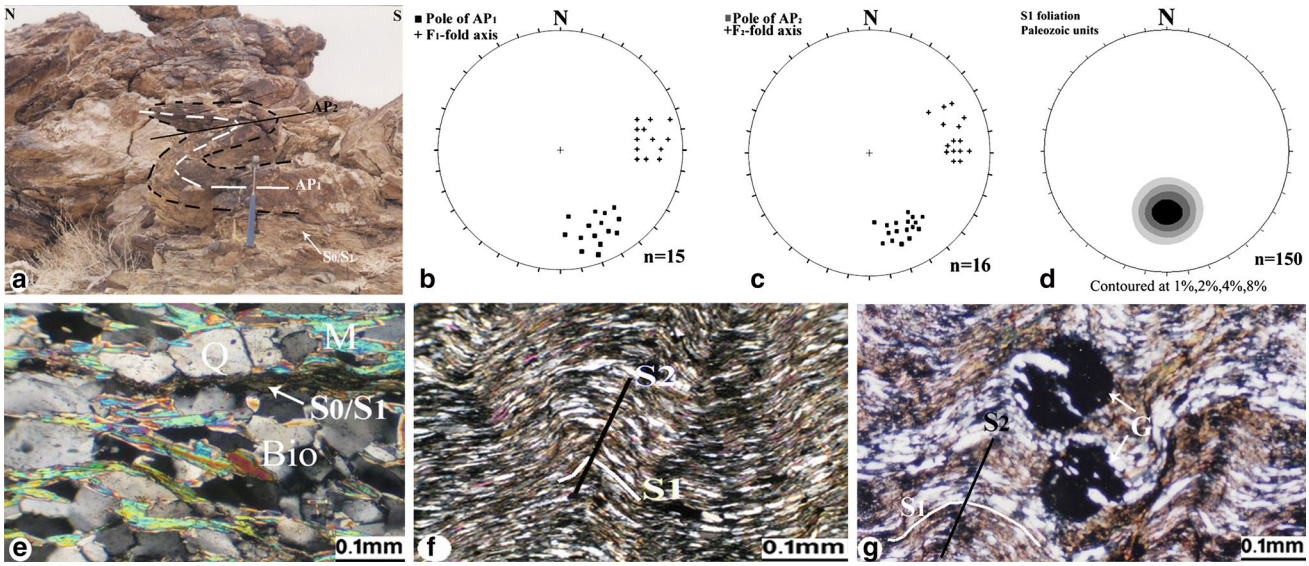

Fig. 3 **a** Type III F1–F2 fold interference pattern in thin marble of the Rutchun complex (Fig. 2) to the east of Kahadan village (**b**, **c**). Lower-hemisphere equal-area stereographic projection of the D_1 and D_2 structural elements exhibited in **a**. **d** Lower-hemisphere equal-area stereographic projection of the S_1 foliation in Paleozoic units. **e**, **f**, **g** Photomicrographs of S_1 foliation that is defined by parallel minerals of muscovite (*M*), biotite (*Bio*), quartz (*Q*) in the green schist from the Routshun Complex and garnet-mica-schist from the Gol-e-Gohar Complexes. **b** The overprinting relation between S_1 foliation (S_1 trending from *left* to *right*) and crenulation cleavage S_2 (S_2 *vertical*). Garnet crystal (*G*) can be interpreted as intertectonic porphyroblast between D_1 and D_2 deformation phases

sandstone S_3 is marked by flattened detrital quartz and the alignment of primary muscovite and chlorite around grains of quartz and feldspar (Fig. 4e). S_3 foliation is generally oriented E–W to NW–SE and dips moderately to the NNE (Fig. 4f).

Five thrust sheets (T_1–T_5) which have been termed the Khabr thrust system are identified in the study area (Figs. 2, 4). Thrust faults have contributed to the complex nature of the outcrop pattern, and they trend NE–SW (T_1) or E–W (T_2–T_3-T_4 and T_5) and dip to the north. The Khabr thrust system contains all the elements that are consistent with hinterland dipping duplexes. The duplexes range in scale from centimeter to several meters (Fig. 5). A variety of features have been produced by these faults. T_2 and T_5 are developed along the southern limbs of folds in the Abkhamosh and Kahdan complexes (Fig. 4), and these complexes have been thrust over older complexes (e.g., the Routshun complex). The appearance of Paleozoic complexes on top of the Jurassic units to the west of Kahdan, and the decreasing thickness of the Gol-e-Gohar complex, reflects development of thrust-related shear zones (e.g., T_3 and T_4, Fig. 2).

The shear zones strike generally E–W and dip moderately N (30°–40°). The upper boundaries to the shear zones are sharp, while the lower boundaries to the shear zones are transitional, and it is difficult to define a distinct boundary. The Shear zones have been named T_2S_1, T_2S_2, T_2S_3, T_4S_1, T_4S_2, T_5S_1 and T_5S_2 (Fig. 6). The main geometrical elements recognized to occur specifically within the shear zones are minor folds and fabrics in deformed rock units. The minor folds are commonly observed in footwall of the thrust shear zones boundary. Two types of minor fold geometry have been distinguished. The geometry of these folds reveals the effect of dip-slip and oblique-slip movements within these thrust-related shear zones. The first asymmetric fold type (Type I) is generated by dip–slip movement and plunges 3°–10° to the west. The fold axes are sub-parallel or at low angles to the local stretching lineation. Folds of this type are best developed within the T2, T4 and shear zones (Fig. 7a–d).

The second fold type (Type II) is asymmetric and vary in their interlimb angle from tight to isoclinal. A typical asymmetric fold is visible between T_3 and T_4 in the northwest of Kahdan, and it appears to plunge obliquely 30° to the NE in parts of the Routshun and Gol-e-Gohar complexes in the map scale (Fig. 7e, f). The mesoscopic scale folds of this type plunge 20°–30° to the NW up to NE, and their axial planes consistently dip moderately to NNW (Fig. 7g, h). This transition in geometry can be attributed to differences in the amount of simple shear. In this model with increase in shear, the fold limbs and axial planes rotate as passive markers until, at very high shear strains, isoclinal folds form with both limbs and axial planes at very low angles to the shear direction (Sanderson 1979). Development of these folds reveals the strike-slip component within the thrust-related shear zones. Shear zones are generated within the thrusts sheets and consist of calc-mylonite,

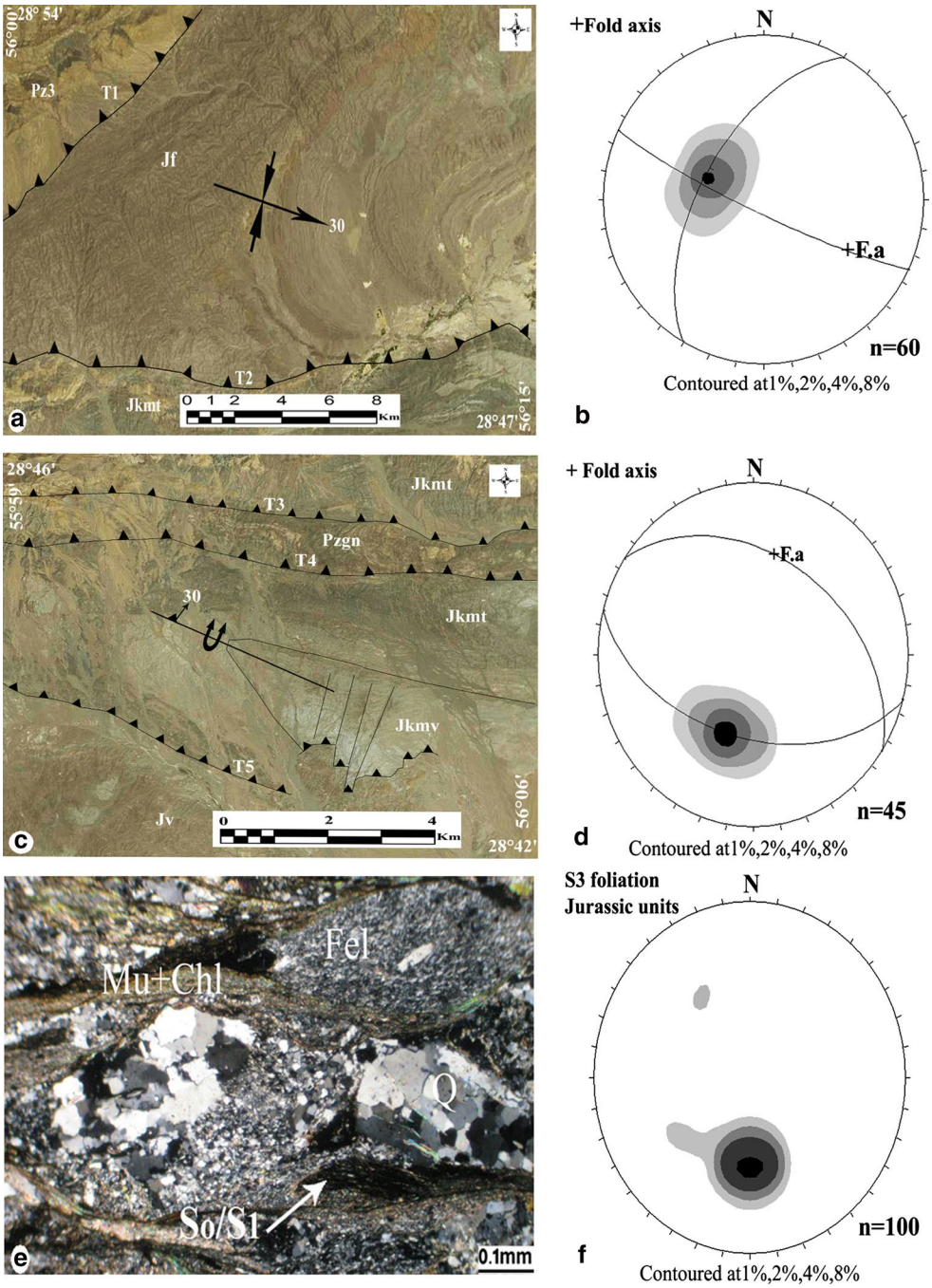

Fig. 4 **a**, **c** Satellite images (from Google Earth) of folds in the Abkhamosh (*Jf*) and Kahdan (*Jkmt*, *Jkmv*) complexes. The southern limbs of these folds became faults in the thrust-related shear zones. **b**, **d** Contoured diagram of poles to bedding onto lower-hemisphere equal-area stereographic projection show that folds in the Abkhamosh Complex are plunging and inclined, and in the Kahdan (*Jkmv*) Complex, they are reclined. Fa is the position of the fold axis. **e** Photomicrograph of poorly developed foliation as a spaced cleavage with muscovite and chlorite (Mu + Chl) that is wrapped around feldspar (*Fel*) and quartz (*Q*). **f** Contoured diagram of S_3 foliation planes (parallel bedding) measured in the Kahdan and Abkhamosh complexes onto lower-hemisphere equal-area stereographic projection. The poles of the S_3 foliation are contoured at 1, 2, 4 and 8 % per 1 % area

quartz-feldspar mylonite, plagioclase-pyroxene (andesite) mylonite and quartz-muscovite mylonite. The foliations display E–W trends and are N-dipping. The stretching lineation in mylonites is defined by the long axes of ellipsoidal grains of different minerals such as quartz, calcite, plagioclase and garnet. In general, stretching lineations trend from N40°W to N 80°W with an intermediate (10°–35°) plunge (Fig. 6).

Microscopic examination of oriented thin sections (normal to foliation and parallel to stretching lineation) from samples collected from the shear zones is shown in Fig. 8. They indicate a dextral sense of shear. The mylonites show a variety of microstructures such as micro-shear zones or microfaults, rotation of porphyroclasts and C′-type shear band cleavage. The porphyroclasts show the two types of microfaults namely "V" pull-apart structures (Fig. 8a, b; Hippert 1993; Samanta et al. 2002) and bookshelf or domino structures (Fig. 8c, d, g; Etchecopar 1977; Ramsay and Huber 1987; Passchier and Trouw 2005). Two types of "V" pull-apart geometry are reported (Hippert 1993): (1) those

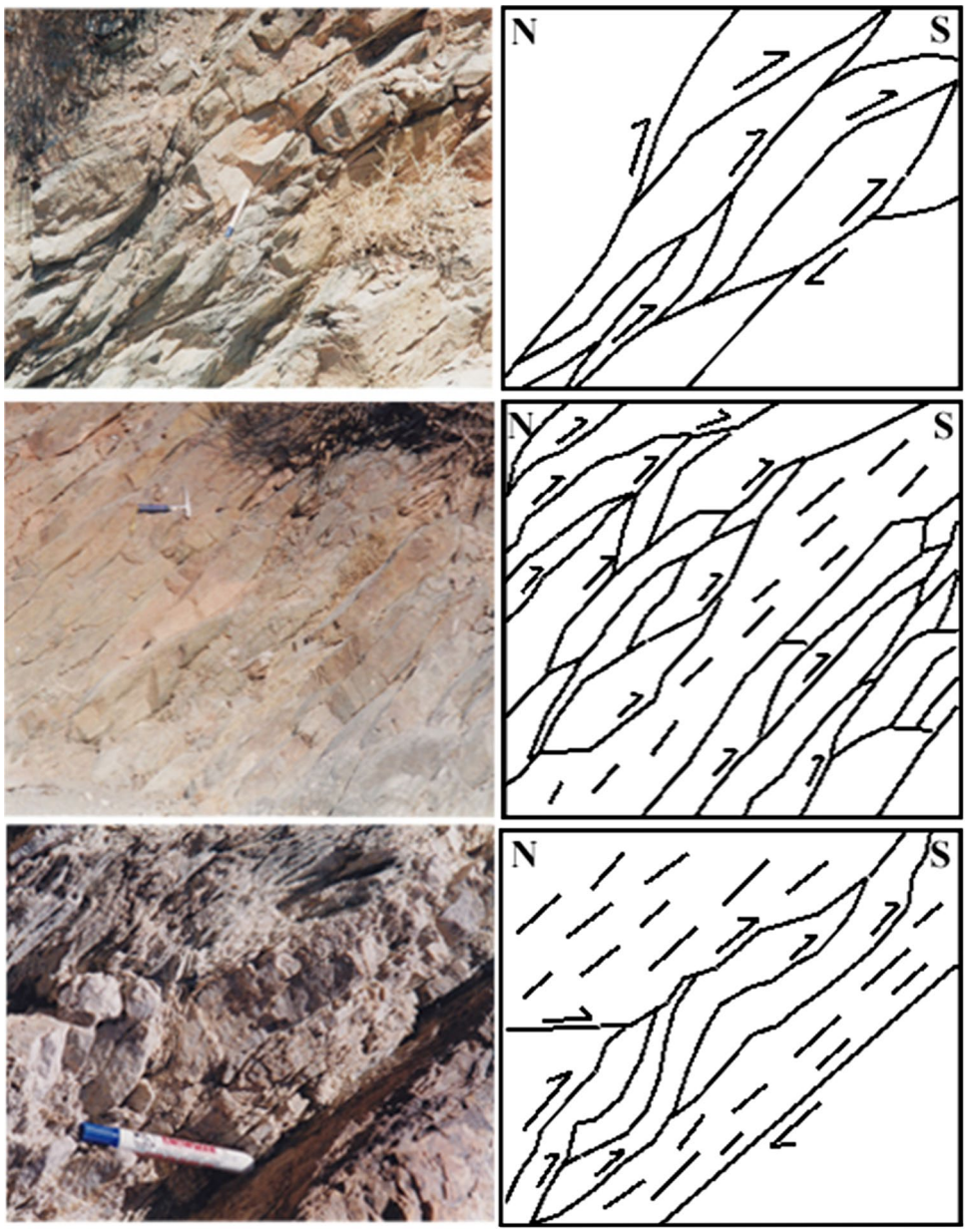

Fig. 5 Photographs of cross sections of flexural-slip duplex structures in the Jkmt units (related to T2 thrust, Fig. 2) showing sigmoidal shape of the horses with a planar or gently curved floor and roof thrust geometry that indicates thrust movement to the south

associated with centrally located sub-parallel fractures (type I) that show offset of fragments (Fig. 8a, b) and (2) off-centered fracture geometry (type II) that characterized by non-parallel wall disposition of fragments. Fig. 8a, b shows the fragments of plagioclase and quartz that separated during rotation, and they form "V" pull-apart microstructures. The "V" pull-apart are filled with fine-grained muscovite and quartz, which display a preferred orientation. In the (Type I) "V" pull-apart microstructures (Fig. 8a, b), the fracture angle (angle of the shear fracture to the normal to the shear direction,) varies from 35° to 40° and the inclination angle (angle the long axis of grain to the shear direction) shows a range from 45° to 60°. The fracture angle and the inclination angle together reflect the effect of the initial orientation of fractures relative to the shear direction (Samanta et al. 2002).

The bookshelf structures in the muscovite and pyroxene porphyroclasts (Fig. 8d, g), respectively, show sets of parallel synthetic and antithetic offsets (Fig. 8d, g). These brittle structures show that fragmented porphyroclasts floating in a ductile matrix undergo fracturing in response to the traction exerted by the flowing matrix (Mandal et al. 2000, 2001; Samanta et al. 2002).

The rotated garnet porphyroclast is identified in samples collected within the T_4 shear zone from garnet schist of the Gol-e-Gohar complex. Fine-grained muscovite and quartz around the ellipsoidal garnet porphyroclast form symmetrical σ-and δ-type systems. The geometry of these

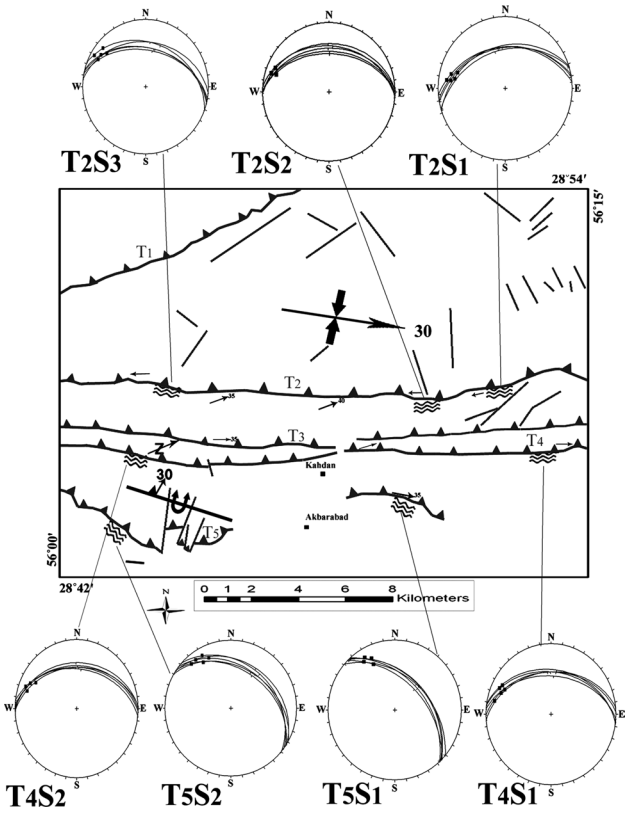

Fig. 6 Generalized structural map of the Khabr area showing the location of shear zones outcrops. Field measurements of the foliations (*great circle*) and stretching lineations (*filled square*) are presented onto lower-hemisphere equal-area projections in the seven shear zone outcrops

porphyroclasts indicates a dextral sense of shear (Schoneveld 1977) (Fig. 8e, f).

A C′-type shear band cleavage (Berthie et al. 1979) is observed in the mica schist mylonite collected from the T_5 shear zone (Fig. 8h). The angle between the C′-planes and the shear zone margin is 30°. S-planes formed within the mica, which has now been strongly altered to chlorite. The geometry of this type of shear band cleavage indicates a dextral sense of shear.

D_4 deformation

The last phase of deformation produced an array of strike-slip faults. These faults are widespread, and they trend in three directions: N10°W to N–S, N30°–45°W and N50°–60°E. There are several indicators in outcrop scales (Fig. 9) that show the shear sense to be both dextral and sinistral. Field observations indicate that the N30°–45°W trending faults have a dextral movement. Some of dextral faults that cut the Eocene–Oligocene units north of T_2-thrust are illustrated in Fig. 9a–c. Traces of sinistral faults with N10°W, N–S trending are identified by displacements of shale and sandstone units north of T_2-thrust (Fig. 9c) and displacement of the Jkmt and JKmv units south of the T_2-thrust (Fig. 9e). The geometry and offset (Fig. 9b–e) show that these fault arrays can be interpreted as a conjugate set of shear fractures, such as antithetic Riedel shears (R'), antithetic X shear and synthetic Riedel shear (R) (Bartlett et al. 1981). These directions of Riedel shears are not consistent with the main stress direction of N20°E in the area. The Khabr area has an E–W somewhat anomalous among the dominant NW–SE trend of the whole Sanandaj–Sirjan zone. Our interpretation is that the Khabr area has been rotated about 45° counterclockwise after generation of all deformation stages described above.

Comparison of deformational domains in the Khabr area with inclined transpression model

Inclined transpression is defined in terms of the simultaneous application of contraction and oblique-slip shearing. Oblique-slip shearing can be further factorized into strike- and dip-slip components. Inclined transpression gives rise to a non-coaxial general flattening deformation and can be represented in terms of which the three end-member plane strain components form the apices of a strain triangle. The strain triangle is not a quantitative tool but can be used to illustrate qualitatively the nature of overall bulk deformation and degree and nature of strain partitioning (Jones et al. 2004). In the following section, the structures of the study area are compared and interpreted using this strain triangle model (Fig. 10).

Contractional domain

The angular unconformity between Paleozoic rocks and Jurassic sediments indicates that deformation in the Paleozoic units developed during the Late Triassic. This phase of deformation is not found in the younger units. In addition, inclined, moderately plunging and reclined folds in the Abkhamosh and Kahdan complexes and the Oligocene–Miocene strata show the dominance of contraction and dip-slip components in the younger deformation stages (Figs. 3, 4, 10a). The younger deformation structures in the Jurassic to Oligocene–Miocene rocks trend E–W, parallel to the earlier Late Triassic structures. On the basis of these structural and the kinematic data, we conclude that the components of contraction had a similar effect during these two different times.

Oblique-slip domain

Deformation in an oblique-slip domain is dominated by N-dipping top-to-the-S thrust-related shear zones. The two types of asymmetric folds generated within the shear zones

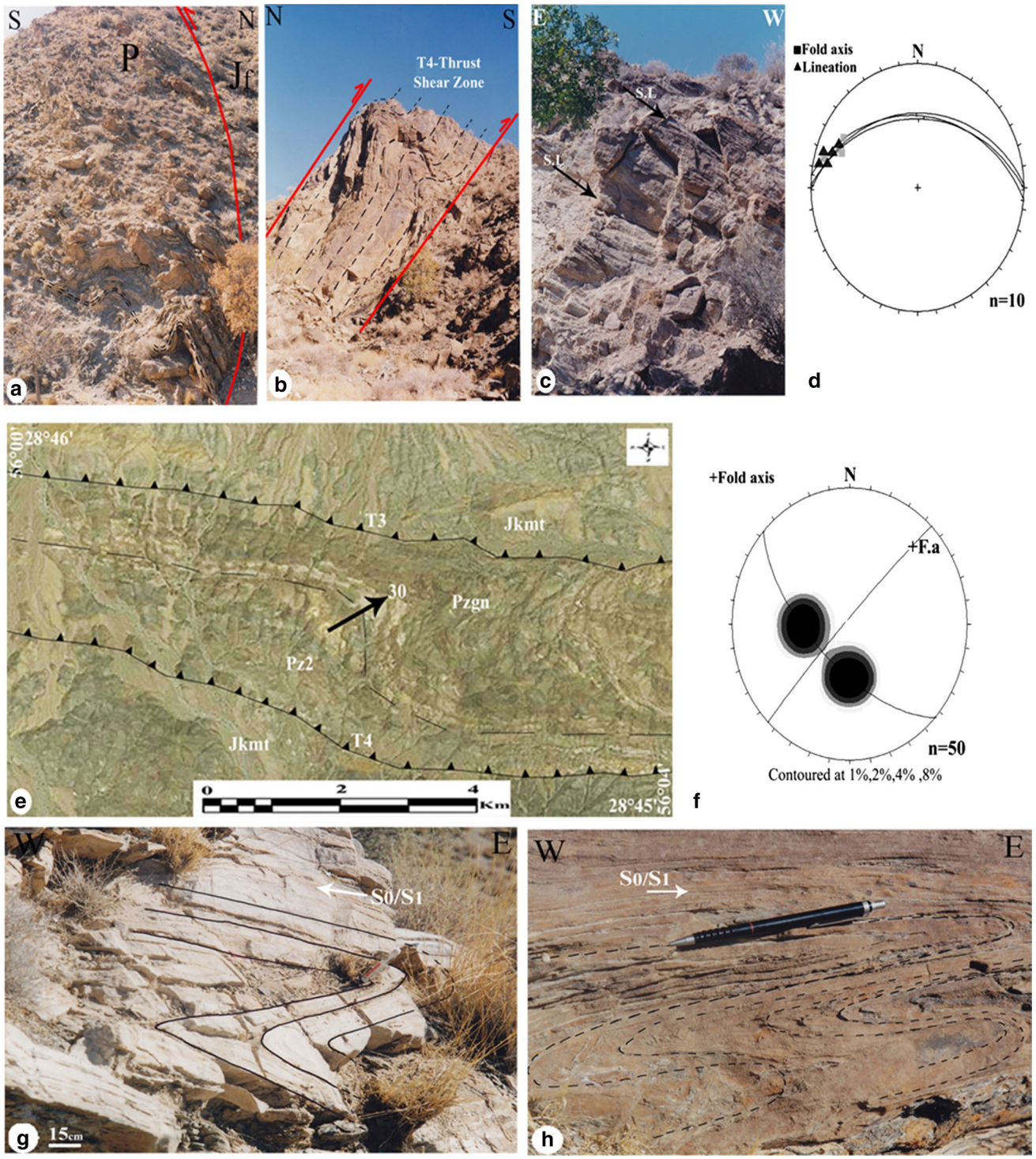

Fig. 7 **a**, **b** Asymmetric folds with strike-parallel hinges. These folds developed as a result of dip-slip shear within the T2 and T4 thrust-related shear zones. *Jf* Jurassic and *P* Paleozoic units. **c** Stretching lineation in calc-mylonite within T_2 shear zones. **d** Lower-hemisphere equal-area stereographic projection of foliation (*great circle*) and lineation (*filled triangle*) and type I fold axes (*filled square*). **e** Satellite image (from Google Earth) of asymmetric fold (Type II) in the Gole-Gohar complex between the T_3 and T_4 thrusts. **f** Contoured diagram of poles to bedding onto lower-hemisphere equal-area stereographic projection shows that this fold is plunging. **g**, **h** Tight to isoclinal type II folds in the thin marble of the Rutchun complex. These folds plunge down dip and show a transition from tight to isoclinal under dextral strike-slip shear in the thrust-related shear zones

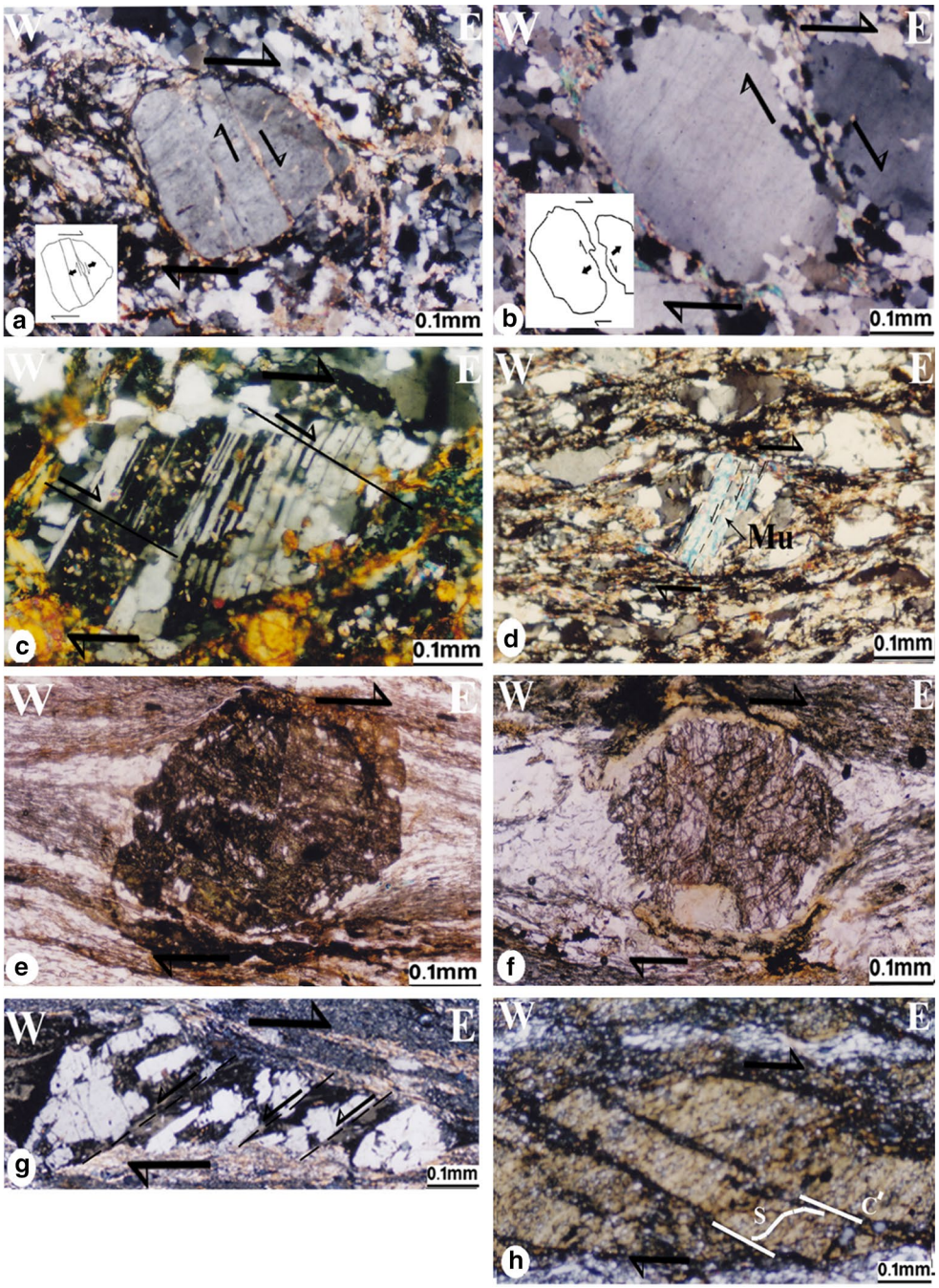

Fig. 8 Microscopic shear sense indicators reveal dextral movement in shear zones in the Khabr area. **a**, **b** The V pull-apart (Type I) structures with antithetically verging fractures walls and synthetic sense of offsetting in feldspar and quartz grains. *Corresponding sketches* highlight the cataclastic structures. *Single-headed arrow* indicates sense of shear. **c** Synthetic microfaults in the plagioclase grain. These indicators reveal a dextral sense of shear in T2 shear zones. **d** Rotation and formation of antithetic shears in a mica porphyroclast. This porphyroclast is separated and sinistrally displaced due to dextral shear. **e**, **f** Rotated garnet porphyroclasts. **e** Symmetrical σ-type and **f** δ-type from garnet schist of the Gol-e-Gohar complex within the T_4S_1 and T_4S_2 shear zones. **g** *S–C′* shear band cleavages in mica schist mylonite that show a dextral sense of shear within the T_5S_1 shear zone. **h** Bookshelf structures or domino fragmented porphyroclast in pyroxene. This porphyroclast internally is broken by parallel fractures. Fragments of pyroxene are separated and sinistrally displaced by dextral shear

show the effect of dip-slip and strike-slip components. The first fold type is related to a dip-slip movement and has a vergence to the S with a hinge parallel to the strike of the thrusts. These folds are well developed in the T_2 and T_5 shear zones (Figs. 7a, b, 10b). The second fold type related to strike-slip is found between the T_3 and T_4 thrusts and are

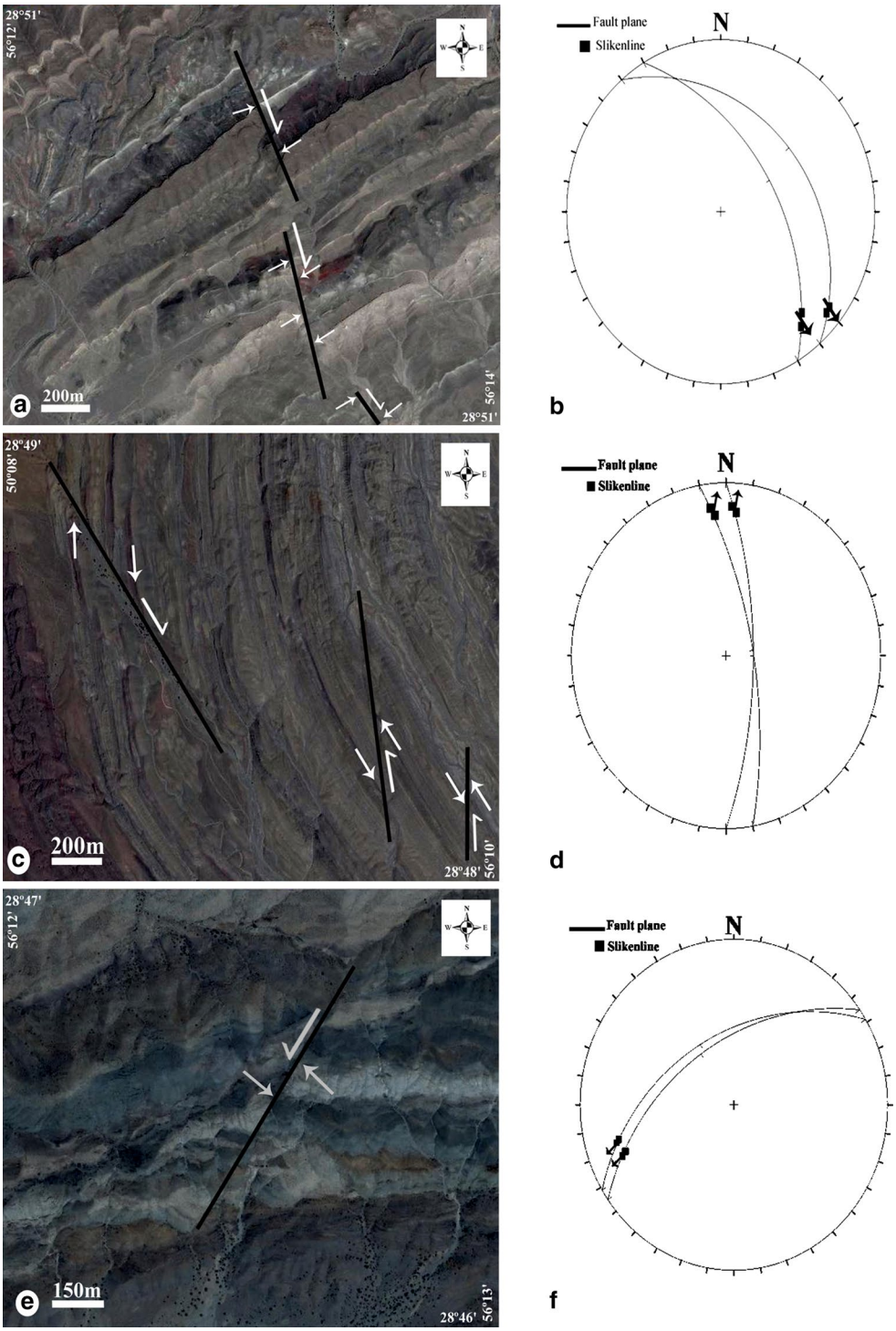

Fig. 9 Satellite images (from Google Earth) of the conjugate shear fractures that are identified by offset shale, sandstone and conglomerate units within the northern limb of Abkhamosh syncline to the north of the T_2-thrust (**a**, **c**, **e**) and offset of Jkmv and Jkmt units to the south of the T_2-thrust lower-hemisphere equal-area projection of measured striations show strike-slip movement for all these faults

asymmetric, steeply plunging, and have dextral "Z" geometries with vergence to the E. The geometry of type II folds shows a transition from close to isoclinal folds (Figs. 7d, e, g, h, 10c).

The geometry of the foliations and lineations within the shear zones reveals the effect of dip- and oblique- slip on the formation of shear zones. Based on the finite strain data from the different area with different lithologies, Sakarinejad (2007) showed that there is no correlation between the magnitude of the strain and the obliquity of the stretching lineation. Analogue experiments modeling a transpression zone with localized non-vertical extrusion reveals that obliquity of the lineation is controlled primarily by the extrusion direction (Czeck and Hudleston 2004). The

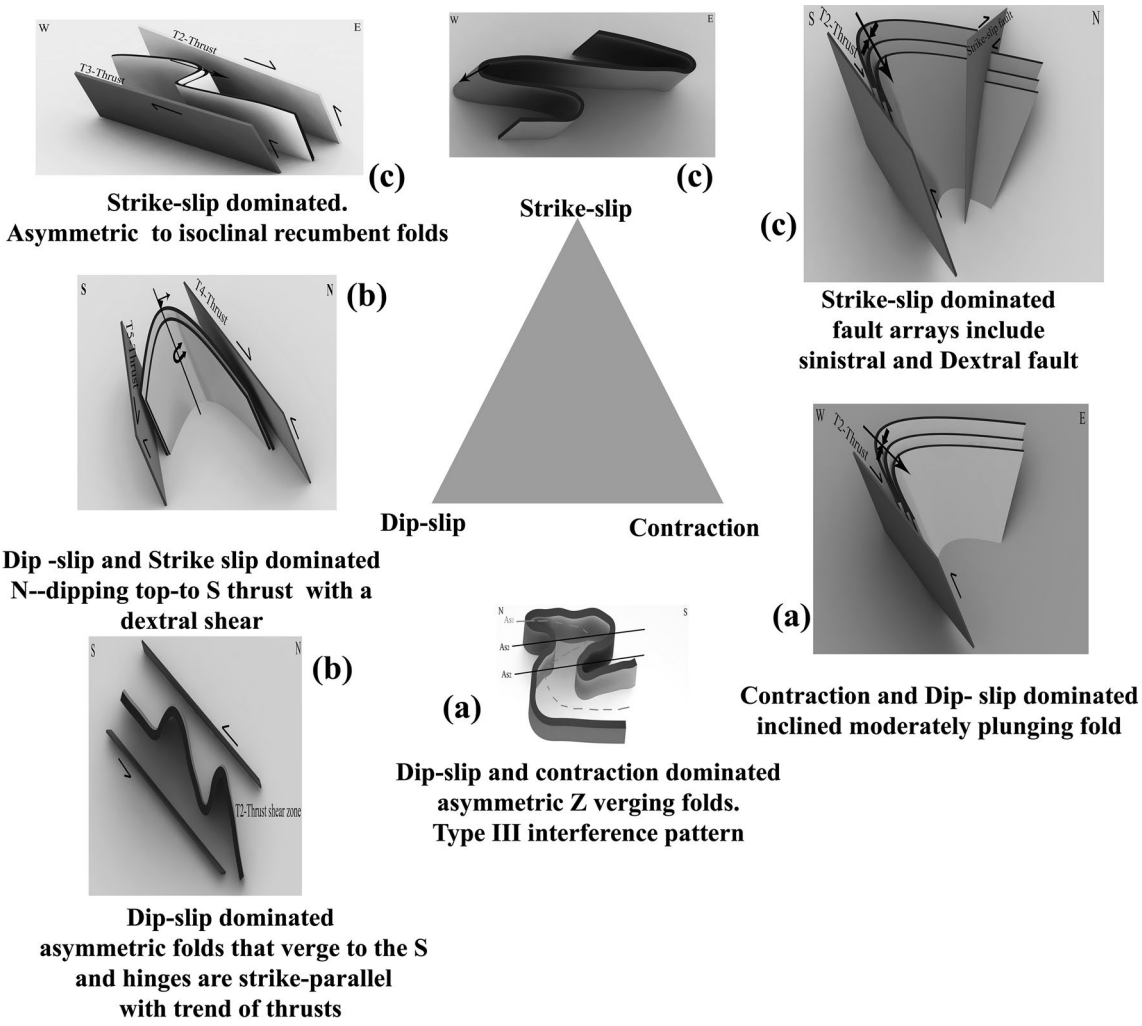

Fig. 10 *Strain triangle* showing the correlation of structures in the Khabr area with the deformational domains (strike-, dip-slip and contraction) in the inclined transpression deformation (see text for explanation of structures)

obliquity of a lineation is mostly controlled by the angle of the non-vertical extrusion direction along the thrust-related shear zones and not the magnitude of the strain or magnitude of simple- or pure-shear components. It is concluded that the shear zones formed during dextral transpression in an inclined convergence thrust wedge.

Strike-slip domain

The continuation of a strike-slip component motion in the last stage of deformation phase caused a set of brittle structures. Structures related to the strike-slip component of motion crop out on the map scale as faults. Strike-slip arrays show both dextral and sinistral displacements. The geometry and offset are consistent with the interpretation that these fault arrays are a conjugate set of shear fractures (Fig. 9).

Correlation of fault data from the Khabr area (SE Sanandaj-Sirjan zone) with the central part of Sanandaj–Sirjan zone (Babaahmadi et al. 2012; Nadimi and Konon 2012; Morley et al. 2009) shows that this strike-slip component of brittle fracturing probably started in the Miocene and continued to the present day.

Conclusions

Deformation in the Khabr area is complex, but geometric and kinematic analyses of the structures show that the deformation is consistent with inclined dextral transpression. The angular unconformity between Paleozoic and Jurassic successions indicates that deformation of the Paleozoic strata occurred in the Triassic. Structures that developed at this time can be interpreted as contractional and related to the subduction of the oceanic crust of Neo-Tethys beneath central Iran. During younger stages, intense folding of the Jurassic, Cretaceous (Abkhamosh and

Kahdan complexes) and Oligocene–Miocene strata took place. Deformation continued, dominated by thrust faulting (thrusts T_1–T_5). T_2 developed along the southern limb of the Abkhamosh syncline, and T_3 along the southern limb of the Kahdan anticline. T_3 and T_4 thrusting juxtaposed older rocks (the Gol-e-Gohar complex) over younger strata. The occurrence within the thrust shear zones of asymmetric folds that have two different orientations (hinges that plunge down dip (Type I) and hinges that are parallel to strike (Type II) and geometry of foliations and lineations and shear sense indicators demonstrate oblique-slip due to a combination of dip- and strike-slip components. The bulk of the deformation at this time consists of a combination of contraction, dip- and strike-slip components. In last stage, a new set of faults was formed in a dominantly dextral strike-slip setting.

We conclude that deformation in the Khabr area started with a contractional component that affected the Paleozoic units. Stratigraphic data reveal that this deformation terminated in the Late Triassic–Early Jurassic. In late deformations (marked by the initiation of the collision of the Afro-Arabian continent and Iranian microcontinent), contractional and dip-slip components resulted in deformation of the Jurassic–Miocene strata and further thrusting. The final deformation in the area was dominated by strike-slip components that produced new arrays of strike-slip fractures. It can be concluded that the structural evolution of this part of the Sanandaj–Sirjan zone occurred under inclined dextral transpression.

Acknowledgments The authors thank Prof. Cosgrove and an anonymous reviewer for their critical comments that greatly contributed to the improvements of the paper and associate Prof. Christopher Fergusson for final editing and some comments. We are thankful to M.M. Baniebrahimi for his help in drawing the 3Dmax images of structures in Fig. 10.

References

Agard P, Omrani J, Jolivet L, Mouthereau F (2005) Convergence history across Zagros (Iran): constraints from collisional and earlier deformation. Int J Earth Sci 94:401–419

Agard P, Omrani J, Jolivet L, Whitechurch H, Vrielynck B, Spakman W, Monie P, Meyer B, Wortel R (2011) Zagros orogeny: a subduction-dominated. Geol Mag 148(5–6):692–725

Ahmadi Khalaji A, Esmaeily D, Valizadeh MV, Rahimpour-Bonab H (2007) Petrology and geochemistry of the granitoid complex of Boroujerd, Sanandaj–Sirjan zone, western Iran. J Asian Earth Sci 29:859–877

Aitchison JC, Ali JR, Davis AM (2007) When and where did India and Asia collide? J Geophys Res Solid Earth 112:B05423. doi:10.1029/2006JB004706

Alavi M (1994) Tectonic of the Zagros Orogenic belt of Iran: new data and interpretation. Tectonophysics 229:211–238

Alavi M (2004) Regional stratigraphy of the Zagros fold–thrust Belt of Iran and its proforeland evolution. Am J Sci 304:1–20

Arfania R, Shahriari S (2009) Role of southeastern Sanandaj–Sirjan zone in the tectonic evolution of the Zagros orogenic belt, Iran. Isl Arc 18(4):555–576

Authemayou C, Chardon D, Bellier O, Malekzadeh Z (2006) Late Cenozoic partitioning of oblique plate convergence in the Zagros fold-and-thrust belt (Iran). Tectonics 25:TC3002. doi:10.1029/2005TC001860

Authemayou C, Bellier O, Chardon D, Benedetti L, Malekzade Z, Claude C, Angeletti B, Shabanian E, Abbassi M (2009) Quaternary slip-rates of the Kazerun and the Main Recent Faults: active strike-slip partitioning in the Zagros fold-and-thrust belt. Geophys J Int 178:524–540

Axen GJ, Fakhari MD, Guest B, Gavillot Y, Stockli DF, Horton BK (2010) Distributed oblique dextral transpression in the High Zagros Mountains, Iran. Tectonic crossroads: evolving orogens of Eurasia–Africa–Arabia. Turkey paper no. 39-5, Middle East Technical University, Ankara

Babaahmadi A, Mohajjel M, Eftekhari A, Davoudian AR (2012) An investigation into the fault patterns in the Chadegan region, west Iran: evidence for dextral brittle transpressional tectonics in the Sanandaj–Sirjan zone. J Asian Earth Sci 43:77–88

Bartlett WL, Friedman M, Logan LM (1981) Experimental folding and faulting of rocks under confining pressure, part IX, wrench faults in limestone layers. Tectonics 79:255–277

Berberian F, Berberian M (1981) Tectono-plutonic episodes in Iran. In: Gupta HK, Delany FM (eds) Zagros, Hindu Kush, Himalaya. Geodynamic evolution, geodynamics series 3. American Geophysical Union, Washington, DC, pp 5–32

Berberian M, King GC (1981) Towards a paleogeography and tectonic evolution of Iran. Can J Earth Sci 18:210–265

Berthie D, Choukroune P, Jegouzo P (1979) Orthogneiss, mylonite and non coaxial deformation of granites: the example of the south American Shear Zone. J Struct Geol 1:31–42

Czeck DM, Hudleston PJ (2004) Physical experiments of vertical transpression with localized nonvertical extrusion. J Struct Geol 26:573–581

Dewey JF, Holdworth RE, Strachan RA (1998) Transpression and transtension zones. In: Holdworth RE, Strachan RA, Dewey JF (ed) Continental transpressional and transtensional tectonics, vol 135. Geological Society, London, Special Publications, pp 1–14

Díaz Azpiroz M, Fernández C (2005) Kinematic analysis of the southern Iberian shear zone and tectonic evolution of the Acebuches metabasites (SW Variscan Iberian Massif). Tectonics 24. doi:10.1029/2004TC001682

Eftekharnejad J (1981) Tectonic division of Iran with respect to sedimentary basins. J Iran Pet Soc 82:19–28 (in Farsi)

Etchecopar A (1977) A plane kinematic model of progressive deformation in a polycrystalline aggregate. Tectonophysics 39:121–139

Falcon NL (1967) Major earth-flexuring in the Zagros Mountain of southwest Iran. J Geol Soci Lond 117:367–376

Ghalamghash J, Nédélec A, Bellon H, Vousoughi Abedini M, Bouchez JL (2009) The Urumieh plutonic complex (NW Iran): a record of the geodynamic evolution of the Sanandaj–Sirjan zone during Cretaceous times—part I: petrogenesis and K/Ar dating. J Asian Earth Sci 35:401–415

Ghasemi H (2001) Petrology, geochemistry and origin of ore deposits in ultramafic and mafic complex of Sikhoran, SE of Iran. Unpublished Ph.D. thesis, University of Tarbiat Modares, Tehran, Iran

Ghasemi A, Talbot J (2006) A new tectonic scenario for the Sanandaj-Sirjan zone (Iran). J Asian Earth Sci 26:683–693

Golonka J (2004) Plate tectonic evolution of the southern margin of Eurasia in the Mesozoic and Cenozoic. Tectonophysics 381:235–273

GSI (1997a) Geological map of Khabr. Geological Survey of Iran, Tehran

GSI (1997b) Geological map of Gol-e-Gohar. Geological Survey of Iran, Tehran
Harland WB (1971) Tectonic transpression in Caledonian Spitzbergen. Geol Mag 108:27–42
Hippert JF (1993) V pull-apart microstructures: a new shear sense indicator. J Struct Geol 15:1393–1404
Jones RR, Holdsworth RE, Bailey W (1997) Lateral extrusion in transpression zones: the importance of boundary conditions. J Struct Geol 19:1201–1217
Jones RR, Holdsworth RE, Clegg Ph, McCaffrey K, Travarnelli E (2004) Inclined transpression. J Struct Geol 26:1531–1548
Lin S, Jiang D, Williams PF (1998) Transpression or transtension zones of triclinic symmetry: natural example and theoretical modeling. In: Holdworth RE, Strachan RA, Dewey JF (eds) Continental transpressional and transtensional tectonics, vol 135. Geological Society, London, Special Publications, pp 41–57
Mahmoodi SH, Corfu F, Masoudi F, Mehrabi B, Mohajjel M (2011) U–Pb dating and emplacement history of granitoid plutons in the northern Sanandaj–Sirjan zone, Iran. J Asian Earth Sci 41:238–249
Mandal N, Chakraborty C, Samanta SK (2000) Boudinage in multilayered rocks under layer-normal compression: a theoretical analysis. J Struct Geol 22:373–382
Mandal N, Chakraborty C, Samanta SK (2001) Control on the failure mode of brittle inclusions hosted in a ductile matrix. J Struct Geol 23:51–66
Mazhari SA, Bea F, Amini S, Ghalamghash J, Molina JF, Montero P, Scarrow JH, Williams IS (2009) The Eocene bimodal Piranshahr massif of the Sanandaj-Sirjan zone, NW Iran: a marker of the end of the collision in the Zagros orogen. J Geol Soc Lond 166:53–69
McQuarrie N, Stock JM, Verdel C, Wernicke BP (2003) Cenozoic evolution of Neo-Tethys and implications for the causes of plate motions. Geophys Res Lett 30. doi:10.1029/2003GL017992
Mohajjel M, Fergusson CL (2000) Dextral transpression in Late Cretaceous continental collision, Sanandaj–Sirjan zone, western Iran. J Struct Geol 22:1125–1139
Mohajjel M, Fergusson CL (2014) Jurassic to Cenozoic tectonics of the Zagros orogen in the northwestern Iran. Int Geol Rev 56(3):263–287
Mohajjel M, Fergusson CL, Sahandi MR (2003) Cretaceous–Tertiary convergence and continental collision, Sanandaj–Sirjan zone, western Iran. J Asian Earth Sci 21:397–412
Mohajjel M, Baharifar A, Moinevaziri H, Nozaem R (2006) Deformation history, micro-structure and P–T–t path in ALS bearing schists, southeast Hamadan, Sanandaj–Sirjan zone, Iran. J Geol Soc Iran 1:11–19
Morley CK, Kongwung B, Julapour AA, Abdolghafourian M, Hajian M, Waples D, Warren J, Otterdoom H, Srisuriyon K, Kazemi H (2009) Structural development of a major late Cenozoic basin and transpressional belt in central Iran: the Central Basin in the Qom–Saveh area. Geosphere 5:1–38
Nadimi A, Konon A (2012) Strike-slip faulting in the central part of the Sanandaj–Sirjan zone, Zagros Orogen, Iran. J Struct Geol 40:2–16
Navabpour P, Angelier J, Barrier E (2007) Cenozoic post-collisional brittle tectonic history and stress reorientation in the High Zagros Belt (Iran, Fars Province). Tectonophysics 432:101–131
Omrani J, Agard P, Whitechurch H, Benoit M, Prouteau G, Jolivet L (2008) Arc magmatism and subduction history beneath the Zagros Mountains, Iran: a new report of adakites and geodynamic consequences. Lithos 106:380–398
Passchier CW, Trouw RAJ (2005) Microtectonics, 2nd edn. Springer, Berlin
Ramsay JG, Huber MI (1987) The technique of modern structural geology. Folds and fractures, vol 2. Academic Press, London
Ricou LE (1994) Tethys reconstructed: plates, continental fragments and their boundaries since 260 Ma from central America to south-eastern Asia. Geodyn Acta (Paris) 7(4):169–218
Robin PYF, Cruden AR (1994) Strian and vorticity patterns in ideally ductile transpression zones. J Struct Geol 16:447–466
Sakarinejad Kh (2007) Quantitative finite strain and kinematic flow analyses along the Zagros transpression zone, Iran. Tectonophysics 442:49–65
Samanta SK, Mandal N, Chakaraborty C (2002) Development of different types of pull-apart microstructures in mylonites: an experimental investigation. J Struct Geol 24:1345–1355
Sanderson RG (1979) The transition from upright to recumbent folding in the Variscan fold belt of southwest England: a model based on the kinematic of simple shear. J Struct Geol 1:171–180
Sanderson DJ, Marchini WRD (1984) Transpression. J Struct Geol 6:449–458
Sarkarinejad Kh, Azizi A (2008) Slip partitioning and inclined dextral transpression along the Zagros Thrust System, Iran. J Struct Geol 30:116–136
Sarkarinejad Kh, Faghih A, Grasemann B (2008) Transpressional deformations within the Sanandaj-Sirjan metamorphic belt (Zagros Mountains, Iran). J Struct Geol 30:818–826
Schoneveld C (1977) A study of some typical inclusion patterns in strongly paracrystalline-rotated garnets. Tectonophysics 39:453–471
Sengor AMC, Natalin BA (1996) Paleotectonics of Asia: fragments of a synthesis. In: Yin A, Harrison TM (eds) The tectonic evolution of Asia. Cambridge University Press, Cambridge, pp 486–640
Shafiei SH, Alavi A, Mohajjel M (2011) Calcite twinning constraints on paleostress patterns and tectonic evolution of the Zagros hinterland: the Sargaz complex, Sanandaj–Sirjan zone, SE Iran. Arab J Geosci 4:1189–1205. doi:10.1007/s12517-010-0140-3
Sheikholeslami MR, Pique A, Mobayen P, Sabzehi M, Bellon H, Emami MH (2008) Tectono-metamorphic evolution of the Neyriz metamorphic complex, Quri-kor-e-sefid area (Sanandaj–Sirjan zone, SW Iran). J Asian Earth Sci 31:504–521
Stöcklin J (1968) Structural history and tectonics of Iran: a review. Am Assoc Pet Geol Bull 52(7):1229–1258
Teyssier C, Tikoff B, Markley M (1995) Oblique plate motion and continental tectonics. Geology 23:447–450
Vernant P, Nilforoushan F, Hatzfeld D, Abbassi MR, Vigny C, Masson F, Nankali H, Martinod J, Ashtiani A, Bayer R, Tavakoli F, Chery J (2004) Present-day crustal deformation and plate kinematics in the Middle East constrained by GPS measurements in Iran and northern Oman. Geophys J Int 157:381–398
Woodruff F, Savin SM (1989) Miocene deepwater oceanography. Paleoceanography 4:87–140